

AD-A076 439

ROCKWELL INTERNATIONAL THOUSAND OAKS CA SCIENCE CENTER F/G 11/2
MICROSTRUCTURALLY DEVELOPED TOUGHENING MECHANISMS IN CERAMICS----ETC(U)
OCT 79 F F LANGE N00014-77-C-0441

UNCLASSIFIED

SC5117.7TR

NL

1 OF 1

AD
A076439



END
DATE
FILMED
12-79
DDC

12 LEVEL II

SC5117.7TR

Copy No. 11

SC5117.7TR

MICROSTRUCTURALLY DEVELOPED TOUGHENING MECHANISMS IN CERAMICS

TECHNICAL REPORT NO. 7

TRANSFORMATION TOUGHENING IN THE
 Al_2O_3/ZrO_2 COMPOSITE SYSTEM

GENERAL ORDER NO. 5117
CONTRACT NO. N00014-77-C-0441

DOCUMENT NO. SC5117.7TR

Prepared for

Office of Naval Research
800 N. Quincy Street
Arlington, VA 22217

F. F. Lange
Principal Investigator

OCTOBER 1979

DDC
RECEIVED
NOV 9 1979
B

Approved for public release; distribution unlimited

Reproduction in whole or in part is permitted
for any purpose of the United States Government



Rockwell International
Science Center

ADA 076439

DDC FILE COPY

79 11 08 071

UNCLASSIFIED

SECURITY CLASSIFICATION OF THIS PAGE (When Data Entered)

| REPORT DOCUMENTATION PAGE | | READ INSTRUCTIONS BEFORE COMPLETING FORM |
|---|-----------------------|--|
| 1. REPORT NUMBER <u>① 0</u> | 2. GOVT ACCESSION NO. | 3. RECIPIENT'S CATALOG NUMBER <u>⑨ 9</u> |
| 4. TITLE (and Subtitle) MICROSTRUCTURALLY DEVELOPED TOUGHENING MECHANISMS IN CERAMICS--Transformation Toughening in the Al ₂ O ₃ /ZrO ₂ Composite System. | | 5. TYPE OF REPORT & PERIOD COVERED Technical Report 1 June 1978 - May 31, 1979 |
| 6. AUTHOR(s) Al sub 2 0 sub 3/ZrO sub 2 F.F./Lange | | 7. PERFORMING ORG. REPORT NUMBER SC5117.7TR TR-7 |
| 8. CONTRACT OR GRANT NUMBER(s) N00014-77-C-0441 | | 14. ④ 15 |
| 9. PERFORMING ORGANIZATION NAME AND ADDRESS Rockwell International Science Center 1049 Camino Dos Rios P.O. Box 1085, Thousand Oaks, CA 91360 | | 10. PROGRAM ELEMENT, PROJECT, TASK AREA & WORK UNIT NUMBERS NR 032-574 (471) |
| 11. CONTROLLING OFFICE NAME AND ADDRESS Office of Naval Research 800 N. Quincy Street Arlington, VA 22217 | | 12. REPORT DATE ⑩ 11 October 1979 |
| 14. MONITORING AGENCY NAME & ADDRESS (if different from Controlling Office) Dr. R.C. Pohanka Office of Naval Research 800 N. Quincy Street Arlington, VA 22217 | | 13. NUMBER OF PAGES 26 |
| 15. SECURITY CLASS. (of this report) Unclassified | | 15a. DECLASSIFICATION/DOWNGRADING SCHEDULE |
| 16. DISTRIBUTION STATEMENT (of this Report) Approved for Public Release, Distribution Unlimited | | |
| 17. DISTRIBUTION STATEMENT (of the abstract entered in Block 20, if different from Report) | | |
| 18. SUPPLEMENTARY NOTES | | |
| 19. KEY WORDS (Continue on reverse side if necessary and identify by block number) Microstructure, Fracture Toughness, Martensitic Transformation, ZrO ₂ , Al ₂ O ₃ | | |
| 20. ABSTRACT (Continue on reverse side if necessary and identify by block number) Three Al ₂ O ₃ /ZrO ₂ composites series, containing 0, 2, and 7.5 mole % Y ₂ O ₃ , respectively, were fabricated. For the Al ₂ O ₃ /ZrO ₂ (+2m/oY ₂ O ₃) series, tetragonal ZrO ₂ was retained from one end-member to the other. Significant increases in fracture toughness and strength were observed for materials in this system. Strengths decreased with increasing temperature. These results are consistent with previous theoretical predictions. ↙ | | |

DD FORM 1473 1 JAN 73 EDITION OF 1 NOV 65 IS OBSOLETE

UNCLASSIFIED

SECURITY CLASSIFICATION OF THIS PAGE (When Data Entered)

389 949

JLB



Rockwell International
Science Center

SC5117.7TR

TRANSFORMATION TOUGHENING IN THE Al_2O_3/ZrO_2 COMPOSITE SYSTEM

F. F. Lange

Structural Ceramics Group
Rockwell International Science Center
Thousand Oaks, CA.

ABSTRACT

Three Al_2O_3/ZrO_2 composite series, containing 0, 2, and 7.5 mole % Y_2O_3 , respectively, were fabricated. For the $Al_2O_3/ZrO_2(+2m/oY_2O_3)$ series, tetragonal ZrO_2 was retained from one end-member to the other. Significant increases in fracture toughness and strength were observed for materials in this system. Strengths decreased with increasing temperature. These results are consistent with previous theoretical predictions.

| | |
|---------------------------------|---|
| ACCESSION for | |
| NTIS | White Section <input checked="" type="checkbox"/> |
| DDC | Buff Section <input type="checkbox"/> |
| UNANNOUNCED | <input type="checkbox"/> |
| JUSTIFICATION _____ | |
| BY _____ | |
| DISTRIBUTION/AVAILABILITY CODES | |
| Dist. AVAIL. and/or SPECIAL | |
| A | |



SC5117.7TR

1.0 INTRODUCTION

A stress-induced, martensitic transformation can be used to increase the fracture toughness of brittle materials based on ZrO_2 .⁽¹⁻⁶⁾ Metastable, tetragonal ZrO_2 is the toughening agent. Transformation to its stable, monoclinic structure in the vicinity of the crack is responsible for the increased fracture toughness.

A previous theoretical study⁽⁷⁾ outlined the thermodynamics concerning the general conditions required to retain tetragonal ZrO_2 and its contribution to fracture toughness. One conclusion was the importance of the elastic properties of the matrix material that constrains the shape change associated with the transformation. That is, both the retention of the metastable phase and its contribution to fracture toughness can be optimized by increasing the elastic modulus of the matrix material. Based on this conclusion, experimental study was directed toward two phase composites in which tetragonal ZrO_2 could be incorporated into a polycrystalline matrix of higher elastic modulus.

The Al_2O_3 - ZrO_2 system was chosen for this study because Al_2O_3 has approximately twice the elastic modulus of ZrO_2 (390 GPa vs 210 GPa) and both phases are compatible with one another.⁽⁸⁾ Claussen⁽⁹⁾ has already demonstrated that Al_2O_3/ZrO_2 polycrystalline composites could be fabricated and, during the course of the present work, he⁽¹⁰⁾ also demonstrated that tetragonal ZrO_2 could be retained in Al_2O_3 in volume fractions up to 0.17.



2.0 EXPERIMENTAL

2.1 Fabrication and Phase Identification

The intent was to fabricate a series of $\text{Al}_2\text{O}_3/\text{ZrO}_2$ material from one end-member to the other and to retain ZrO_2 in its tetragonal structure. Initial studies indicated that within the range of fabrication parameters investigated, pure, tetragonal ZrO_2 could only be retained in volume fractions <0.15 . Based on phase retention studies in the $\text{ZrO}_2\text{-Y}_2\text{O}_3$ system,⁽⁶⁾ additions of 2 mole % Y_2O_3 to the $\text{Al}_2\text{O}_3/\text{ZrO}_2$ composite powder were used to retain the tetragonal phase from one end-member to the other.

Three composite series were fabricated for this study: one containing pure ZrO_2 with volume fractions up to 0.20, one containing $\text{ZrO}_2 + 2\text{m/o Y}_2\text{O}_3^*$ in which tetragonal ZrO_2 was retained from one end-member to the other, and one containing $\text{ZrO}_2 + 7.5\text{m/oY}_2\text{O}_3$ in which cubic ZrO_2 was the second phase. The latter composite series was used for base line information where transformation toughening was not a phenomena associated with the material's mechanics.

Sub-micron powders were used.[†] Y_2O_3 was introduced as yttrium nitrate.[§] Composite powders were mixed by ball-milling with methanol and Al_2O_3 balls in a plastic container. All powders were dried; those containing

*m/o = mole %, v/o = volume %

† Al_2O_3 : Lindy B, Union Carbide Corp.; ZrO_2 : Zircas Corp.

§Research Chemicals Inc.



SC5117.7TR

yttrium nitrate were calcined at 400°C for 4 hrs. Densification was achieved by hot-pressing. Most Y_2O_3 containing compositions were hot-pressed at 1600°C/2 hrs; compositions containing 0.8 and 1.0 volume fraction $ZrO_2(+2m/oY_2O_3)$ were hot-pressed at 1400°C in order to achieve a smaller grain size which allowed the retention of tetragonal ZrO_2 . The non-yttria composites were hot-pressed at 1500°C, again to achieve a smaller grain size for optimizing the retention of tetragonal ZrO_2 . The pure Al_2O_3 end-member was hot-pressed at 1400°C to achieve a grain size comparable to the two-phase materials (the introduction of one end-member into the other limited grain growth).

Archimedes' technique was used to measure density of the 5 cm diameter hot-pressed billets. Specimens were cut, ground and polished* prior to phase identification by x-ray diffraction analysis. Two-theta scans between 27° to 33° were used to estimate the tetragonal/monoclinic ZrO_2 ratio and scans between 55° to 62° were used to confirm either the tetragonal or the cubic ZrO_2 phase.

2.2 Mechanical Measurements

Young's modulus (E) of selected compositions was measured at room temperature by the resonance technique in two modes of vibration: flexural (9kHz) and extensional (60 kHz).

*Surface damage caused by cutting and grinding causes the surface to transform. Polishing decreases the depth of the transformed surface layer.



SC5117.7TR

The critical stress intensity factor (K_C) was measured on polished specimens by using the indentation technique and the function

$$K_C = \frac{H\sqrt{d}}{3(H/3E)^{0.4}} f(c/d) \quad (1)$$

developed by Evans and Charles.⁽¹¹⁾ The hardness (H) was measured at a load of 20 kgm. The half-diagonal (d) of the pyramidal indent and half-crack length (c) were used with Young's modulus and the experimentally obtained function ⁽¹¹⁾ [f(c/d)] to compute K_C . Three measurements were made for each material.

Flexural strength measurements were obtained in four-point bending (inner span: 1.22 cm, outer span: 2.54 cm) on diamond cut specimens (approximately 0.32 x 0.32 cm cross sectional) finished with a 220 grit diamond grinding wheel.



3.0 RESULTS

3.1 Fabrication and Phase Identification

Table 1 lists the fabrication conditions for the compositions reported here and their respective average properties. Densities of the $\text{Al}_2\text{O}_3/\text{ZrO}_2(+2\text{m/oY}_2\text{O}_3)$ materials obeyed the rule of mixtures for the end-members (Al_2O_3 and tetragonal ZrO_2); this indicated that theoretical density was achieved during fabrication. With the exception of the 60, 80, and 100% $\text{ZrO}_2(+2\text{m/oY}_2\text{O}_3)$ materials, tetragonal ZrO_2 was fully retained in this series. High proportions of tetragonal ZrO_2 could only be retained in the $\text{Al}_2\text{O}_3/\text{ZrO}_2$ (pure) series for volume fractions of $\text{ZrO}_2 < 0.10$.* The 20v/o ZrO_2 composition in this series was friable, indicative of its high monoclinic content and suggestive of a highly microcracked material.

Figure 1 illustrates microstructures of polished surfaces typical of all the $\text{Al}_2\text{O}_3/\text{ZrO}_2$ compositions (cracks observed are those purposely propagated from the hardness indent). In general, the minor phase appears uniformly dispersed. The observed agglomeration of the minor phase in occasional groups of 2-5 grains indicates that the dispersion could be improved. The average grain size for the composite materials was dependent on the fabrication temperature, viz. $\sim 0.2 \mu\text{m}$ at 1400°C , $\sim 0.5 \mu\text{m}$ at 1500°C and $\sim 1 \mu\text{m}$ at 1600°C . The

*It should be noted that phase identification was obtained from polished surfaces. Although polishing is effective in removing much of the damaged, transformed surface layer produced during machining, the tetragonal content of the subsurface material could be higher than reported in Table 1.



average grain size of the end-members hot-pressed at 1400°C was $\sim 2 \mu\text{m}$ for Al_2O_3 and $\sim 0.5 \mu\text{m}$ for ZrO_2 .

3.2 Hardness

Figure 2 illustrates the Vickers (20 kgm) hardness as a function of composition, suggesting a linear rule of mixtures for the $\text{Al}_2\text{O}_3/\text{ZrO}_2(2\text{m}/\text{oY}_2\text{O}_3)$ series. The highly microcracked, 20v/o ZrO_2 (pure) composition is the exception to this behavior; its hardness is considerably less. Observations of the material adjacent to the hardness indent suggest that the indenter pushed the microcracked material aside as it extended into the surface.

3.3 Young's Modulus

Figure 3 reports the Young's modulus obtained from the two resonance techniques as a function of composition.

3.4 Critical Stress Intensity Factor

Figure 4 reports K_{Ic} as a function of composition for the three series of materials. The elastic modulus vs composition data shown in Fig. 3 was used with the experimental parameters (H,d,c) to compute K_{Ic} according to Eq.(1).

It should be pointed out here that the K_{Ic} values calculated for the $\text{Al}_2\text{O}_3/\text{ZrO}_2$ (pure) series (Fig. 4b) may be somewhat large due to the monoclinic contents of these materials. Namely, their monoclinic content suggests the



SC5117.7TR

presence of microcracks that would lower Young's Modulus from those shown in Fig. 3, which were used to calculate K_C . As shown by Eq. (1), the relation between K_C and E is weak, e.g., a 20% decrease in E will only produce ~10% decrease in the calculated value of K_C . Thus, although the presence of monoclinic ZrO_2 in these materials might lower E (due to the presence of microcracks), the decrease in K_C from that reported is expected to be small. This effect is most significant for the 20% ZrO_2 (pure) composition where direct evidence for preexisting microcracks exists, viz. its friable nature and low hardness.

3.4 Strength

Flexural strength was determined as a function of composition for the $Al_2O_3/ZrO_2(+2m/oY_2O_3)$ series and as a function of temperature for the composition containing 23.9v/o $ZrO_2(+2m/oY_2O_3)$.

Strength vs composition results are plotted in Fig. 5. Specimens containing >45v/o $ZrO_2(+2m/oY_2O_3)$ were observed to contain one or two large through cracks of undetermined origin; strengths of these materials are not represented in Fig. 5. Results for strength vs temperature for the Al_2O_3/ZrO_2 (23.9v/o + 2m/o Y_2O_3) material are illustrated in Fig. 6.



4.0 ANALYSIS

4.1 Retention of Tetragonal ZrO₂

Theory⁽⁷⁾ indicates that a critical size exists, below which a particle of tetragonal ZrO₂ can be constrained from transforming by an elastic matrix. The critical particle (or grain) size can be increased by increasing the elastic properties of the constraining matrix. In previous work,⁽⁶⁾ a sufficiently small particle size could not be fabricated to retain pure, tetragonal ZrO₂ in a ZrO₂ constraining matrix. This work indicated that a particle size <0.2 μm would be required for a ZrO₂ constraining matrix. The current work has shown that pure, tetragonal ZrO₂ can be retained for an average particle size of 0.5 μm when the elastic modulus of the constraining matrix is increased to ~390 GPa (i.e., a composite of Al₂O₃ + small volume fractions of ZrO₂). A similar result has been obtained by Claussen.⁽¹⁰⁾ Less of the tetragonal ZrO₂ is retained in the Al₂O₃/ZrO₂ (pure) series as the volume fraction of the ZrO₂ is increased. The increased ZrO₂ content decreases the elastic modulus of the composite and thus shifts the critical particle size to smaller values than those achieved during fabrication. These observations are consistent with the theory relating phase retention to the elastic properties of the constraining matrix.

Theory⁽⁷⁾ also indicates that the critical size can be increased by increasing the differential chemical free energy ($\Delta G_{t \rightarrow m}^{\text{chem}}$) for ZrO₂(t) + ZrO₂(m) reaction. Alloying ZrO₂ with Y₂O₃ increases $\Delta G_{t \rightarrow m}^{\text{chem}}$ as evident from the lowering of the transformation temperature for Y₂O₃ additions up to eutectoid



SC5117.7TR

composition at ~3m/o.⁽⁶⁾ In the previous study, the critical grain particle size of tetragonal $ZrO_2(+2m/oY_2O_3)$ was determined to be 0.2 μm . The current study shows that the critical particle size can be increased to at least 1 μm with the higher elastic modulus of the Al_2O_3/ZrO_2 constraining matrix. Also note that as the $Al_2O_3/ZrO_2(+2m/oY_2O_3)$ composition approaches the ZrO_2 end-member, a large fraction of the tetragonal $ZrO_2(+2m/oY_2O_3)$ could not be retained by fabricating at 1600°C which produces a particle (or grain) size of 1 μm . In order to achieve a greater amount of phase retention, the fabrication temperature was decreased to 1400°C so that a grain size of 0.2 μm could be obtained. These observations are consistent with the theory⁽⁷⁾ relating phase retention to the free energy change of the martensitic reaction.

4.2 Critical Stress Intensity Factor

A previous theoretical study⁽⁷⁾ concerning the contribution of the stress-induced transformation to fracture toughness resulted in two expressions for the critical stress intensity factor, which represent the lower and upper bounds expected for K_{Ic} . The lower bound solution assumes that the transformation does not exhibit a stress hysteresis; this implies that the size of the process zone at the crack front is relatively independent of temperature. The expression for the lower-bound solution is

$$K_{Ic}^{lb} = [K_0^2 - A E_c V_d]^{1/2}, \quad (2)$$

where

$$A = \frac{2\Delta G_{t \rightarrow m}^{chem}}{(1-\nu_c^2)}$$



SC5117.7TR

K_0 is the critical stress intensity factor for the composite material without the transformation, $\Delta G_{t+m}^{\text{chem}}$ is the differential chemical free energy for the $\text{ZrO}_2(t) \rightarrow \text{ZrO}_2(m)$ reaction, E_c and ν_c are Young's Modulus and Poisson's ratio for the composite, respectively, V_d is the volume fraction of the retained tetragonal ZrO_2 and R is the size of the process zone.

The upper bound solution assumes that the stress-induced transformation at the crack front is irreversible due to a stress hysteresis effect. With this assumption, the size of the process zone (r) depends on temperature and K_0 . The upper bound K_c solution has the form

$$K_c^{\text{ub}} = K_0 (1 + BE_c V_p)^{-1/2} \quad (3)$$

where

$$B = \frac{2\Delta G_{t+m}^{\text{chem}} \left(\frac{\Delta V}{V}\right)^2}{[2\pi(1 - \nu_c^2)\Delta G_{t+m}^{\text{chem}} + U_{se}^0]^2}$$

U_{se} is the strain energy and $\Delta V/V$ is the volume change associated with the transformation.

Comparisons of the upper and lower bound solutions with the experimental data were made by calculating the constants A and B in Eqs (2) and (3), respectively, by using the experimental data for the 45v/o ZrO_2 (+2m/o Y_2O_3) composition. These constants were used along with the experimental E_c (Fig. 3) and K_0 (Fig. 4a) for the $\text{Al}_2\text{O}_3/\text{ZrO}_2(7.5\text{m/oY}_2\text{O}_3)$ series to calculate K_c^{ub} and K_c^{lb} as a function of V_p . As seen in Fig. 4, the lower bound solution agrees with the experimental data for $V_p < 0.6$.



SC5117.7TR

Further comparison can be made with the lower bound solution by using Whitney's (12) thermodynamic data for pure ZrO_2 . By assuming the same value of $\delta\Delta G/\delta T$ reported by Whitney for pure ZrO_2 and an unconstrained transformation temperature of $800^\circ C$ for the $ZrO_2(+2m/oY_2O_3)$, $\Delta G_{C \rightarrow m}^{chem}(25^\circ C) = -193 \times 10^6 J/m^3$. Substituting this value into Eq. (2) along with the other experimental factors, the radius of the process zone (R) is calculated to be $1 \mu m$. This calculation suggests that the transformation depth on the crack surface is $1 \mu m$ which is the approximate particle size of the retained, tetragonal ZrO_2 in these materials. The agreement between the calculated zone size and the particle size adds some confidence to the theoretical results for the lower bound solution.

The maximum in the K_{IC} data for the Al_2O_3/ZrO_2 (pure) series can be explained by the decreasing retention of tetragonal ZrO_2 for $V_{ZrO_2} > 0.10$. That is, the maximum K_{IC} was obtained for the composition in which the retention was a maximum. Claussen⁽⁹⁾ also observed maximum in his K_{IC} data for two series of Al_2O_3/ZrO_2 (pure) materials over a similar range of V_{ZrO_2} . For his data, the maximum K_{IC} shifted to a higher volume fraction for the smaller particle size series where greater retention of the tetragonal phase is expected from theory. From these observations, it can be concluded that tetragonal ZrO_2 is the toughening agent and K_{IC} can be optimized by retaining the maximum content of this phase.



4.3 Strength vs Composition

The strength data presented in Fig. 5 has been analyzed to determine its dependence on the experimental K_C values. In this analysis, it was assumed that the crack size distribution responsible for failure remained unchanged from material to material. With this assumption, the strength of each material should be related by their respective critical stress intensity factors:

$$\sigma_2 = \left(\frac{K_2}{K_1}\right)\sigma_1 \quad (4)$$

This relation was used with the average strength and K_C for the pure Al_2O_3 to obtain the broken line in Fig. 5. As shown, three of the original five sets of data were in good agreement with this analysis, but two of the data sets (viz $V_p = 0.182$ and 0.295) were higher than predicted.

Pascoe and Garvie⁽¹³⁾ have shown that surface compressive stress arises in materials containing metastable, tetragonal ZrO_2 when the transformation at the surface is induced by an abrasion process. The volume increase associated with transformed surface layer gives rise to the compressive stresses. Since each set of strength specimens was independently surface ground, it was suspected that several of these sets (the two that resulted in the higher values) may have received surface damage to imparted sufficient surface compressive stresses to increase their strength. To test this hypothesis, a small task was initiated to examine the effect of surface abrasion on strength. Although the principal results of this task will be reported



SC5117.7TR

elsewhere,⁽¹⁴⁾ it was shown that if the abrasively ground specimens were annealed at 1300°C to eliminate the transformed surface layer, the average strength was lowered to that expected from Eq. (4). These data are shown by the open triangle in Fig. 5.

It can be concluded that the strength of the $\text{Al}_2\text{O}_3/\text{ZrO}_2(+2\text{m/oY}_2\text{O}_3)$ composite materials increases proportionally to their increase in K_C as expected. Additional strengthening can be obtained by compressive stressing the surfaces through abrasion. Studies are currently underway to characterize and optimize the abrasion phenomena.

4.4 Strength vs Temperature

Strength data in Fig. 6 were analysed in the same manner as described by Eq. (4). Eq.(2) was used to obtain K_C as a function of temperature. Whitney's results (12) for $\Delta G_{\rightarrow m}^{\text{chem}}$ vs temperature for pure ZrO_2 were used to determine the temperature dependence of the factor A in Eq. (2) with an assumed unconstrained transformation temperature of 800°C for $\text{ZrO}_2(+2\text{m/oY}_2\text{O}_3)$. The results of this analysis are represented as the solid line in Fig. 6.

As shown in Fig. 6, the lower bound solution for K_C results in near perfect agreement with strength vs temperature data over the range of 25° to 1000°C. At temperatures <25°C, agreement is poor - which may be due to either an increase process zone size at these lower temperatures (suggesting that the



Rockwell International
Science Center

SC5117.7TR

upper bound K_C solution may be valid at lower temperatures) or some other currently unexplained reason.



5.0 CONCLUSIONS

It has been demonstrated that the critical stress intensity factor and the strength of polycrystalline Al_2O_3 can be significantly increased by incorporating tetragonal ZrO_2 . Fabrication conditions required to retain the tetragonal phase at room temperature indicate a critical particle size must not be exceeded. The critical particle size appears to be related to the elastic properties of the constraining matrix and the alloy additions to ZrO_2 as indicated by theory.

The fracture toughness is related to the amount of retained tetragonal phase, i.e., tetragonal ZrO_2 is the toughening agent. When the present data are compared to similar data obtained for the $\text{ZrO}_2(\text{cubic})/\text{ZrO}_2$ (tetragonal) composite series,⁽⁶⁾ it can be shown that greater gains in K_{IC} are observed with the higher elastic modulus of the $\text{Al}_2\text{O}_3/\text{ZrO}_2$ constraining matrix as predicted by theory. Although more fundamental thermodynamic data and direct measurements of the process zone size are needed, the current K_{IC} and strength data indicate that the process zone size is independent of composition and temperature.

Regardless of the views expressed relating theory and experiment, it should be noted that materials fabricated for this study are some of the strongest ceramics and that surface abrasion is not detrimental. These bottom line results strongly suggest that transformation toughening should be pursued for other systems within the framework of present and improved theoretical direction.



REFERENCES

1. R. C. Garvie, R. H. Hennick and R. T. Pascoe, *Nature* 258, 703 (1975).
2. R. C. Garvie and R. T. Pascoe, *Processing of Crystalline Ceramics*, ed. by H. Palmour III, R. F. Davis and T. M. Hare, p. 263, Plenum Press (1978).
3. D. L. Porter and A. H. Heuer, *J. Am. Ceram. Soc.* 60, 183 (1977); *ibid.* 280 (1977).
4. T. K. Gupta, J. H. Bechtold, R. C. Kuznichi, L. H. Cadoff and B. R. Rossing, *J. Mat. Sci.* 12, 2421 (1977).
5. T. K. Gupta, F. F. Lange and J. H. Bechtold, *J. Mat. Sci.* 13, 1464 (1978).
6. F. F. Lange, "Transformation Toughening in the ZrO_2 (Cubic)/ ZrO_2 (tetragonal) Composite System," to be published: ONR Rept #3, Contract N00014-77-C-0441, July 1978.
7. F. F. Lange, "Stress-Induced Phase Transformations: Theory of Phase Retention and Fracture Toughness," ONR Rept #6, Contract N00014-77-C-0441, Oct. 1979.
8. E. M. Levin, C. R. Robbins, and H. F. McMurdie, "Phase Diagrams for Ceramists, 1969 Supplement," The American Ceramic Soc., 1969.
9. N. Claussen, *J. Am. Ceram. Soc.* 59 [1-2], 49 (1976).
10. N. Claussen, *ibid* 61 [1-2], 85 (1978).
11. A. G. Evans and E. A. Charles, *J. Am. Ceram. Soc.* 59 [7-8], 371-2 (1976).
12. E. D. Whitney, *J. Am. Cerma, Soc.* 45, 612 (1962).
13. R. T. Pascoe and R. C. Garvie, "Ceramic Microstructures '76," ed by R. M. Fulrath and J. A. Pask, Westview Press p.774, 1977.
14. D. J. Green and F. F. Lange, to be published.



ACKNOWLEDGEMENTS

The careful technical services of M. G. Metcalf are deeply appreciated. The author also wishes to acknowledge the valuable discussions with D. R. Clarke and D. J. Green. Thanks are due B. R. Tittman and E. H. Cirlin for the elastic modulus measurements. This work was supported by the Office of Naval Research under Contract N00014-77-C-0441.



SC5117.7TR

TABLE I
FABRICATION CONDITIONS, PHASE CONTENT AND PROPERTIES OF Al_2O_3/ZrO_2 COMPOSITES

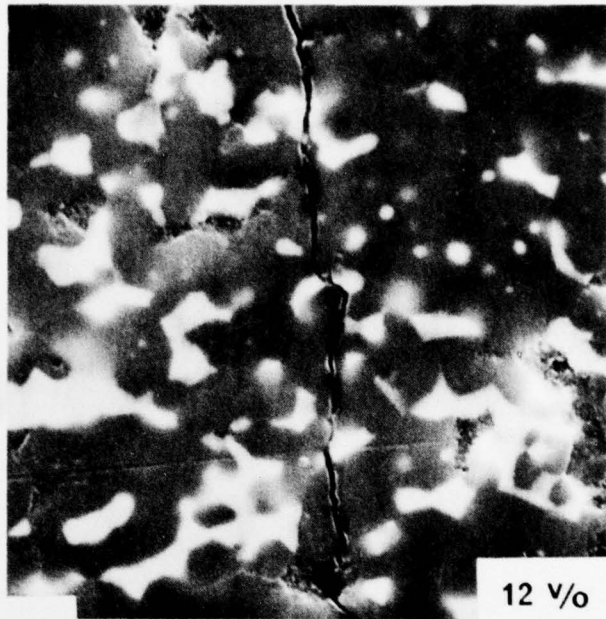
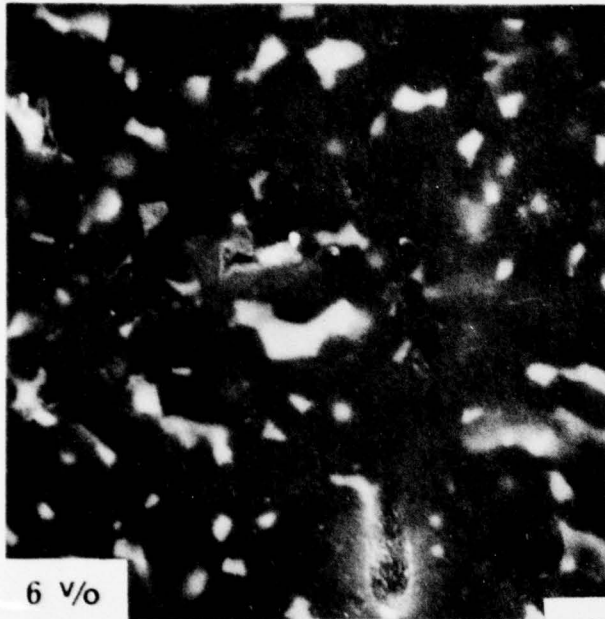
| v/o ZrO_2 | m/o Y_2O_3 | Fabrication Condition | Density (gm/cm^3) | % ZrO_2^* phrase | H (GPa) | E (GPa) | Kc ($MPa m^{1/2}$) |
|---------------------------------------|--------------|-----------------------|-----------------------|--------------------|---------|---------|----------------------|
| $Al_2O_3/ZrO_2(+2m/oY_2O_3)$ Series | | | | | | | |
| 0 | - | 1400°C/2hr | 3.98 | - | 17.6 | 390 | 4.89 |
| 6 | 2 | 1600°C/2hr | 4.12 | 100t | 16.8 | - | 5.97 |
| 12.3 | 2 | 1600°C/2hr | 4.26 | 100t | 15.9 | - | 6.22 |
| 18.2 | 2 | 1600°C/2hr | 4.38 | 100t | 16.1 | 356 | 6.58 |
| 23.9 | 2 | 1600°C/2hr | 4.50 | 100t | 16.4 | - | 6.38 |
| 29.5 | 2 | 1600°C/2hr | 4.62 | 100t | 15.7 | - | 7.43 |
| 45.0 | 2 | 1600°C/2hr | 4.89 | tr m | 15.1 | 291 | 8.12 |
| 60.0 | 2 | 1600°C/2hr | 5.24 | ~95t | 13.7 | - | 7.45 |
| 80.0 | 2 | 1400°C/2hr | 5.57 | ~85t | 12.6 | 237 | 6.79 |
| 100.0 | 2 | 1400°C/2hr | 6.01 | ~80t | 11.6 | 210 | 6.62 |
| Al_2O_3/ZrO_2 (pure) Series | | | | | | | |
| 7.5 | - | 1500°C/2hr | 4.12 | ~90t | 17.2 | - | 5.88 |
| 10.0 | - | 1500°C/2hr | 4.15 | ~80t | 15.8 | - | 6.73 |
| 12.5 | - | 1500°C/2hr | 4.22 | ~70t | 16.9 | - | 6.21 |
| 15.0 | - | 1500°C/2hr | 4.25 | ~50t | 17.3 | - | 5.71 |
| 20.0 | - | 1600°C/2hr | - | <20t | 10.1 | - | (5.25) |
| $Al_2O_3/ZrO_2(+7.5m/oY_2O_3)$ Series | | | | | | | |
| 20.0 | 7.5 | 1600°C/2hr | 4.46 | 100c | 15.8 | - | 4.54 |
| 40.0 | 7.5 | 1600°C/2hr | 4.89 | 100c | 15.9 | - | 3.75 |
| 60.0 | 7.5 | 1600°C/2hr | 5.28 | 100c | 15.0 | - | 3.50 |
| 80.0 | 7.5 | 1600°C/2hr | 5.63 | 100c | 14.3 | - | 3.14 |
| 100.0 | 7.5 | 1600°C/2hr | 5.95 | 100c | 11.4 | - | 3.90 |

t = tetragonal
c = cubic
trm = trace monoclinic



FIGURES

- Fig. 1 SEM micrographs of polished surfaces of $\text{Al}_2\text{O}_3/\text{ZrO}_2(+2\text{m/oY}_2\text{O}_3)$ composites at ZrO_2 volume fractions of 0.053, 0.123, 0.45 and 0.80. Al_2O_3 is dark phase.
- Fig. 2 Vicher's Hardness (measured at 20 kgm) for the true composite series.
- Fig. 3 Young's Modulus vs composition for the $\text{Al}_2\text{O}_3/\text{ZrO}_2(+2\text{m/oY}_2\text{O}_3)$ series.
- Fig. 4 a) Critical stress intensity factor vs composition for the $\text{Al}_2\text{O}_3/\text{ZrO}_2(+2\text{m/oY}_2\text{O}_3)$ (circles) and the $\text{Al}_2\text{O}_3/\text{ZrO}_2(+7.5\text{m/oY}_2\text{O}_3)$ series (squares).
b) Critical stress intensity factor vs composition for the $\text{Al}_2\text{O}_3/\text{ZrO}_2(\text{pure})$ series.
- Fig. 5 Flexural strength vs composition for the $\text{Al}_2\text{O}_3/\text{ZrO}_2(+2\text{m/oY}_2\text{O}_3)$ series.
- Fig. 6 Flexural strength vs temperature for the $\text{Al}_2\text{O}_3/\text{ZrO}_2(25.9 \text{ v/o} + 2\text{m/oY}_2\text{O}_3)$ material.



2um

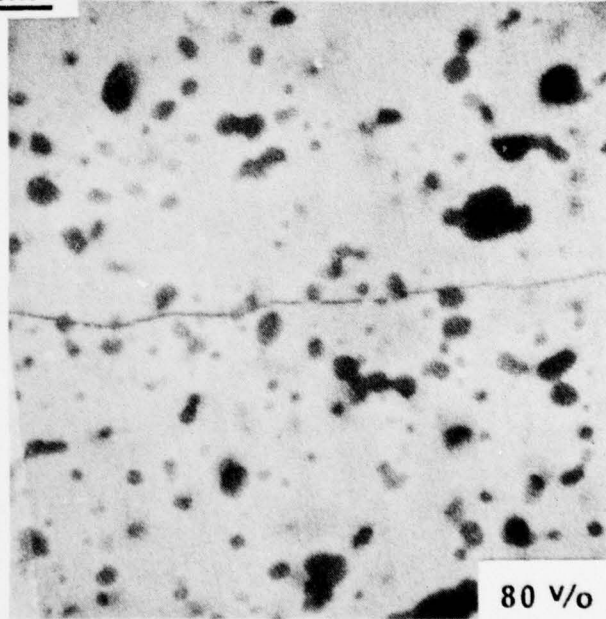
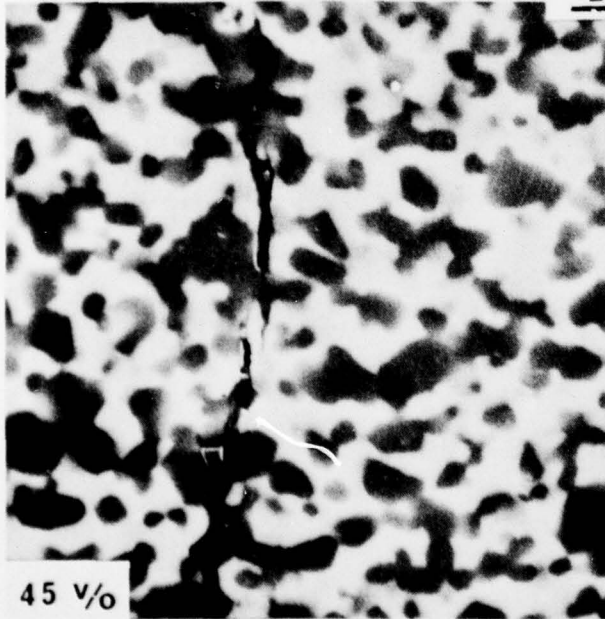


Fig. 1



SC5117.7TR

SC79-5969

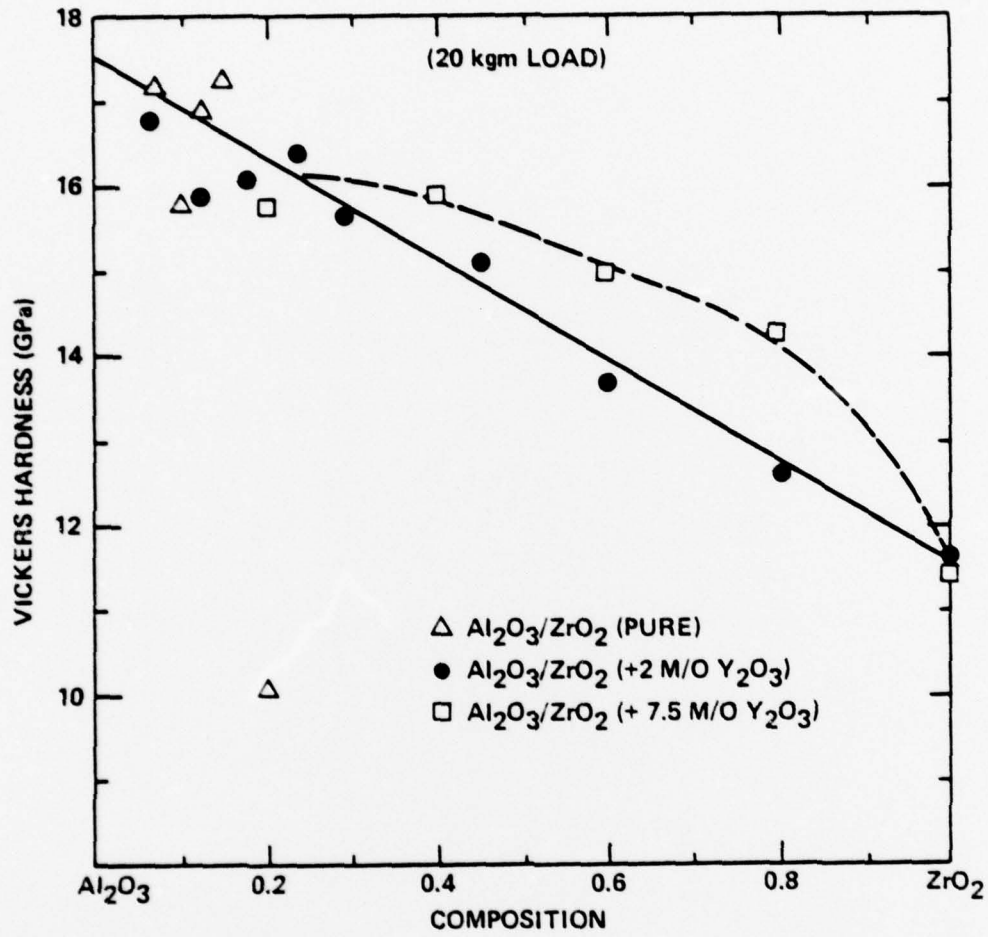


Fig. 2



SC5117.7TR

SC79-5968

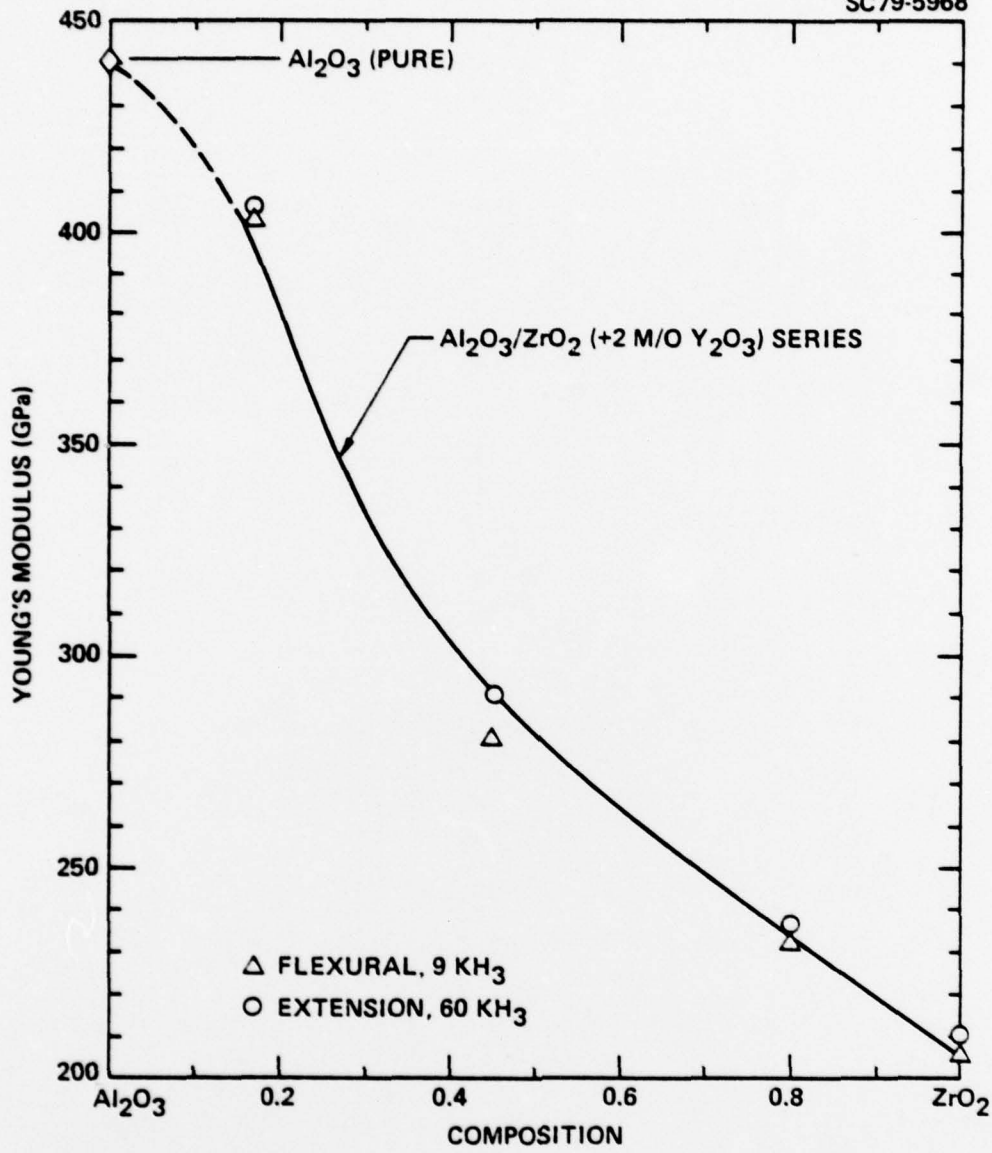


Fig. 3



SC5117.7TR

SC79-5970

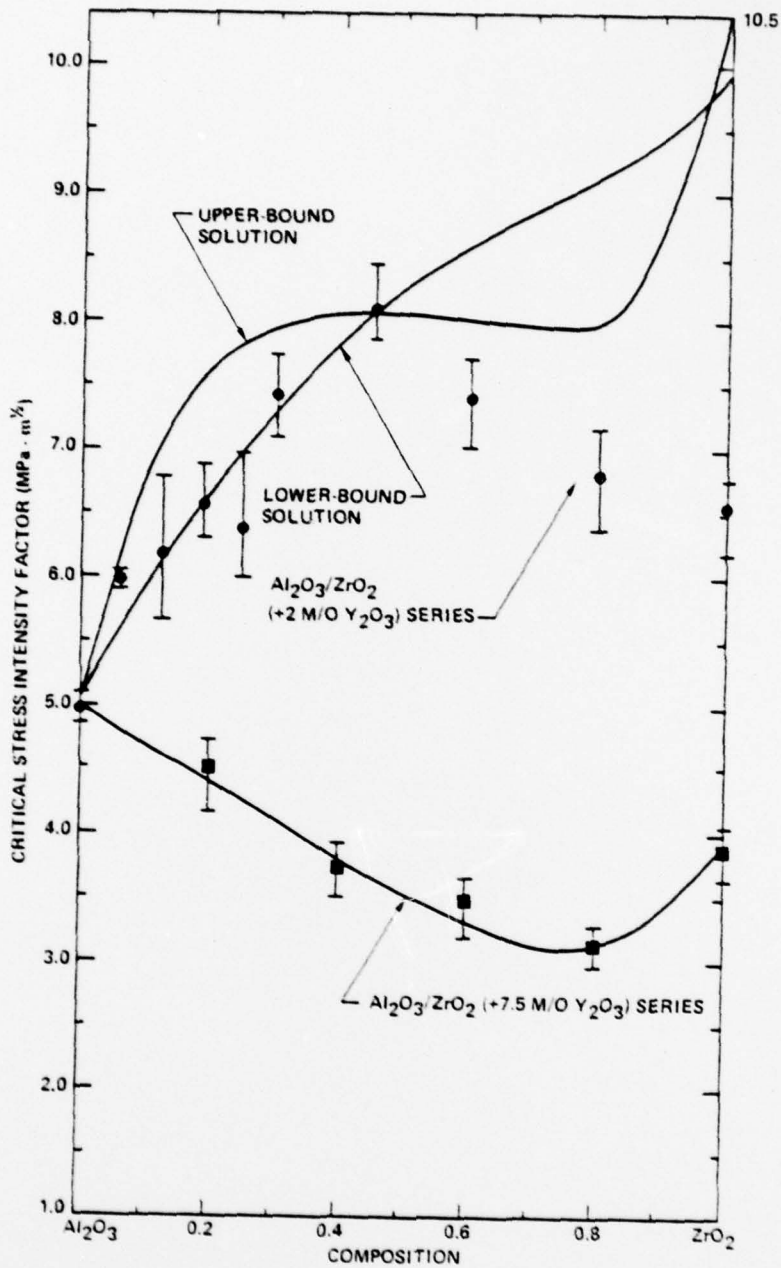


Fig. 4a



SC5117.7TR

SC79-5972

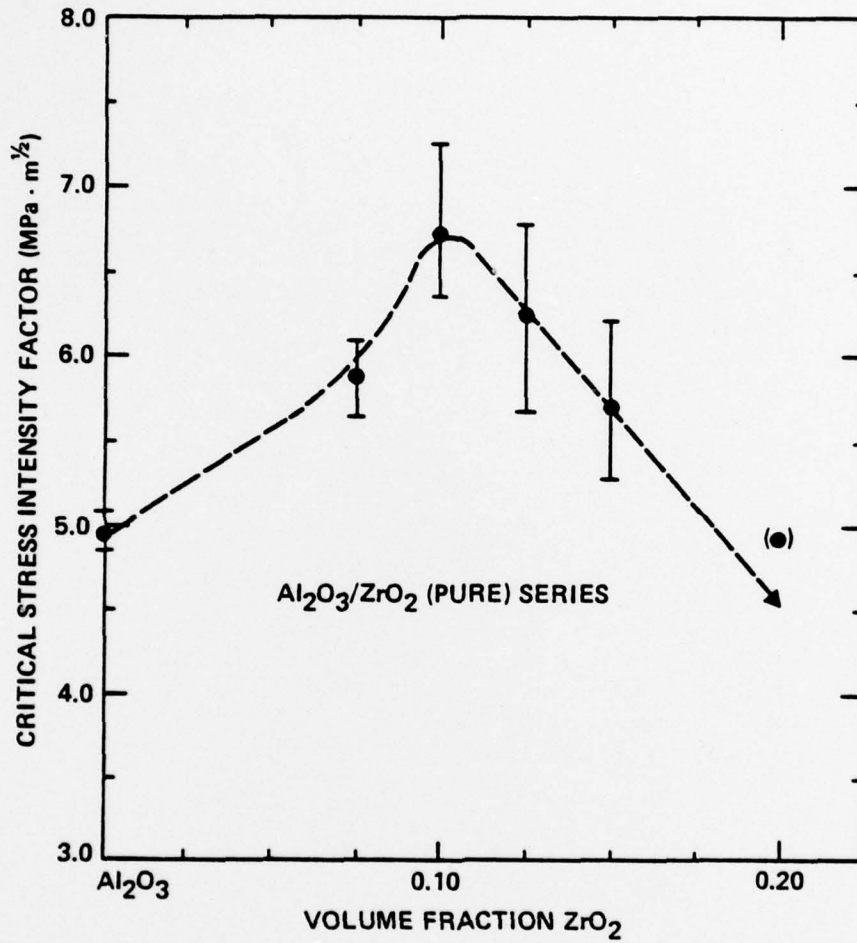


Fig. 4b



SC79-5971

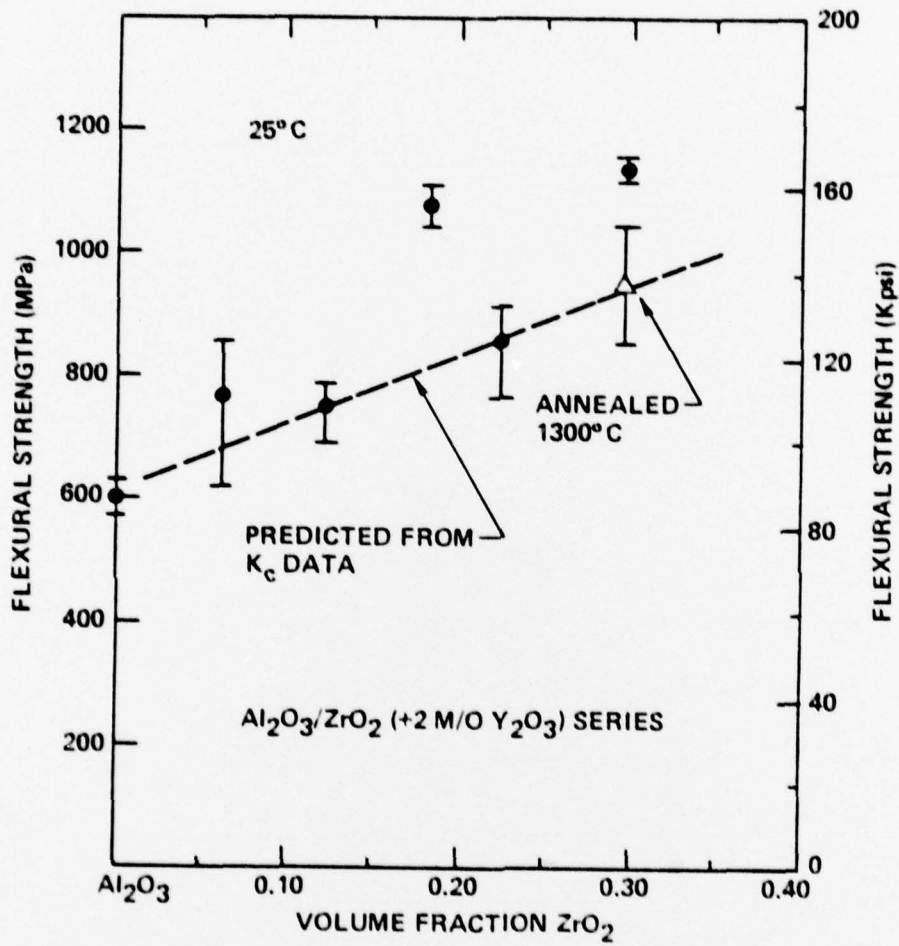


Fig. 5



SC5117.7TR

SC79-5967

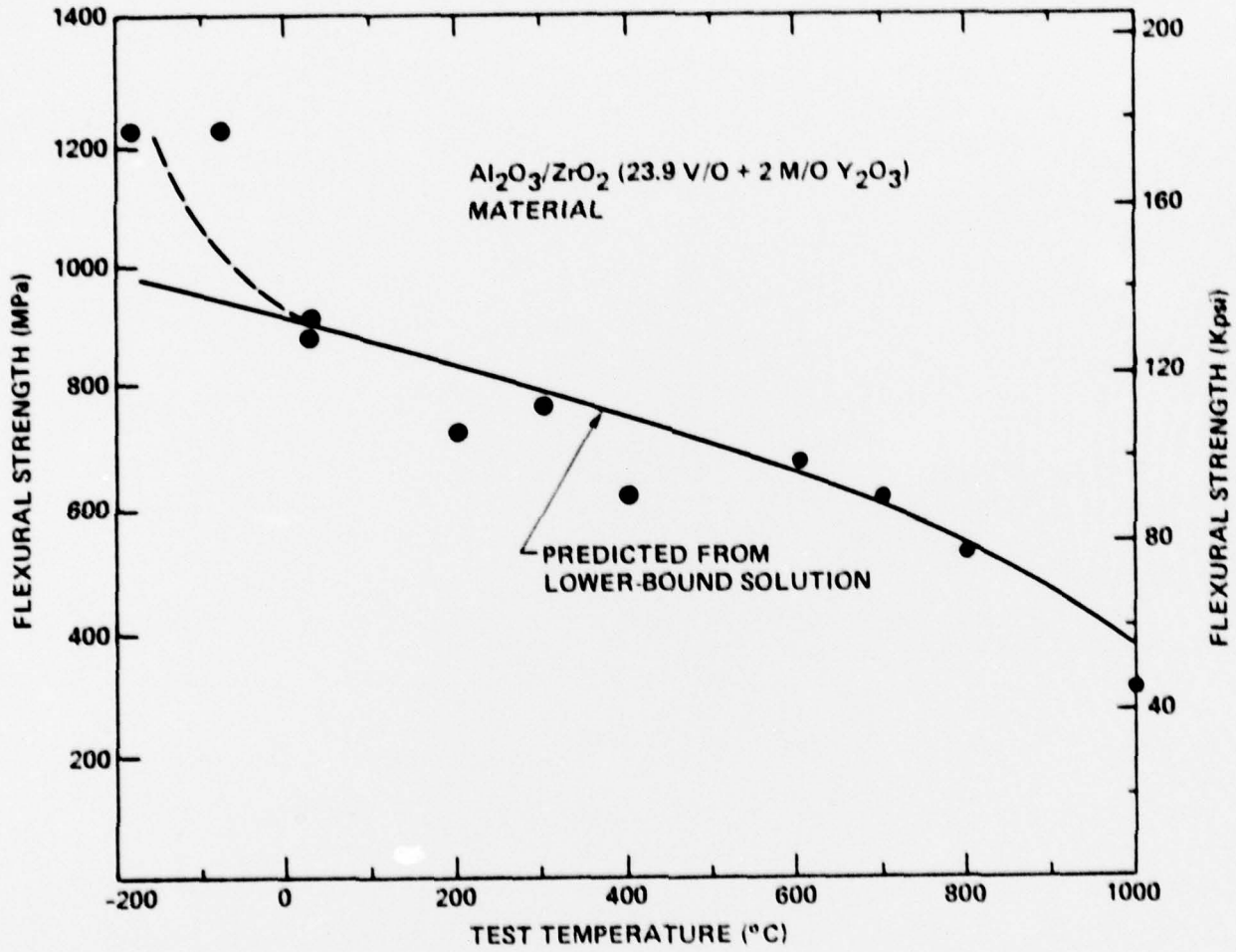


Fig. 6